

Can ultrastrong coupling change ground-state chemical reactions?

Luis A. Martínez-Martínez,¹ Raphael F. Ribeiro,¹ Jorge Campos-González-Angulo,¹ and Joel Yuen-Zhou¹

¹*Department of Chemistry and Biochemistry, University of California San Diego, La Jolla, California 92093, United States*

(Dated: June 14, 2017)

Recent advancements on the fabrication of organic micro- and nanostructures have permitted the strong collective light-matter coupling regime to be reached with molecular materials. Pioneering works in this direction have shown the effects of this regime in the excited state reactivity of molecular systems and at the same time have opened up the question of whether it is possible to introduce any modifications in the electronic ground energy landscape which could affect chemical thermodynamics and/or kinetics. In this work, we use a model system of many molecules coupled to a surface-plasmon field to gain insight on the key parameters which govern the modifications of the ground-state Potential Energy Surface (PES). Our findings confirm that the energetic changes *per molecule* are determined by effects which are essentially on the order of single-molecule light-matter couplings, in contrast with those of the electronically excited states, for which energetic corrections are of a collective nature. Still, we reveal some intriguing quantum-coherent effects associated with pathways of concerted reactions, where two or more molecules undergo reactions simultaneously, and which can be of relevance in low-barrier reactions. Finally, we also explore modifications to nonadiabatic dynamics and conclude that, for our particular model, the presence of a large number of dark states yields negligible effects. Our study reveals new possibilities as well as limitations for the emerging field of polariton chemistry.

I. INTRODUCTION

The advent of nano- and microstructures which enable strong confinement of electromagnetic fields in volumes as small as $1 \times 10^{-7} \lambda^3$ [1], λ being a characteristic optical wavelength, allows for the possibility of tuning light-matter interactions that can “dress” molecular degrees of freedom and give rise to novel molecular functionalities. Several recent studies have considered the effects of strong coupling (SC) between confined light and molecular states, and its applications in exciton harvesting and transport [2, 3], charge transfer [4], Bose-Einstein condensation [5–7], Raman [8, 9] and photoluminescence [10, 11] spectroscopy, and quantum computing [12–14], among many others [15–17]. Organic dye molecules are good candidates to explore SC effects due to their unusually large transition dipole moment [18–21]. More recently, it has been experimentally and theoretically shown that the rates of photochemical processes for molecules placed inside nanostructures can be substantially modified [4, 22–25]. The underlying reason for these effects is that the SC energy scale is comparable to that of vibrational and electronic degrees of freedom, as well as the coupling between them [26]; this energetic interplay nontrivially alters the resulting energetic spectrum and dynamics of the molecule-cavity system. It is important to emphasize that in these examples, SC is the result of a collective coupling between a single photonic mode and $N \gg 1$ molecules; single-molecule SC coupling is an important frontier of current research [27], but our emphasis in this work will be on the N molecule case. Since the energy scale of this collective coupling is larger than the molecular and photonic linewidths, the resulting eigenstates of the system have a mixed photon-matter character. Un-

derstanding these so-called *polariton* states is relevant to develop a physical picture for the emerging energy landscapes which govern the aforementioned chemical reactivities. More specifically, Galego and coworkers [26] have recently provided a comprehensive theoretical framework to explain the role of vibronic coupling and the validity of the Born-Oppenheimer (BO) approximation in the SC regime, as well as a possible mechanism for changes in photochemical kinetics afforded by polaritonic systems [24]; another theoretical study that focused on control of electron transfer kinetics was given by Herrera and Spano [4]. Using a model of one or two molecules coupled to a single mode in a cavity, Galego and coworkers noticed that some effects on molecular systems are collective while others are not; similar findings were reported by Cwik and coworkers using a multimode model and N molecules [28]. While prospects of photochemical control seem promising, it is still a relatively unexplored question whether ground-state chemical reactivity can be altered via polaritonic methods, although recently, George and coworkers have shown a proof of concept of such feasibility using vibrational SC [23]. Along this line, ultrastrong coupling regime (USC) seems to also provide the conditions to tune the electronic ground-state energy landscape of molecules and in turn, modify not only photochemistry, but ground-state chemical reactivity. Roughly speaking, this regime is reached when $\Omega/\hbar\omega_0 \geq 0.1$, Ω being the (collective) SC of the emitter ensemble to the electromagnetic field and $\hbar\omega_0$ the energy gap of the molecular transition [29]. Under USC, the “nonrotating” terms of the light-matter Hamiltonian acquire relevance and give rise to striking phenomena such as the dynamical Casimir effect [30, 31] and Hawking radiation in condensed matter systems [31]. Furthermore, recent experimental advances have rendered the USC regime feasible in circuit

QED [32], inorganic semiconductors [33, 34], and molecular systems [35, 36], thus prompting us to explore USC effects on ground-state chemical reactivity.

In this article, we address how this reactivity can be influenced in the USC by studying a reactive model system consisting of an ensemble of thiocyanine molecules strongly coupled to the plasmonic field afforded by a metal, where each of the molecules can undergo cis-trans isomerization by torsional motion. The theoretical model for the photochemistry of the single thiocyanine molecule has been previously studied in the context of coherent control [37]. As we will show, the prospects of controlling ground-state chemical reactivity or non-adiabatic dynamics involving the ground state are not promising for this particular model, given that the alterations of the corresponding PES are negligible on a per-molecule basis. However, we notice the existence of salient quantum-coherent features associated with concerted reactions that might be worth considering in models featuring lower kinetic barriers.

This article is organized as follows: in the Theoretical Model section, we describe the polariton system and its quantum mechanical Hamiltonian. In Methods, we describe the methodology to perform the relevant calculations and understand the effects of polariton states on the ground-state PES of the molecular ensemble. In Results and Discussion we describe our main findings, and finally, in the Conclusions section, we provide a summary and an outlook of the problem.

II. THEORETICAL MODEL

To begin with, we consider a thiocyanine derivative molecule (Fig. 1c) and approximate its electronic degrees of freedom as a quantum mechanical two-level system. To keep the model tractable, this electronic system is coupled to only one vibrational degree of freedom R , namely, the torsion along the bridge of the molecule (Fig. 1c) along which cis-trans isomerization occurs. The mathematical description of the PES of the ground and excited states (Fig. 1a) as well as the transition dipole moment as a function of the reaction coordinate (Fig. 1b) have been obtained from Ref. [37]. The adiabatic representation of the electronic states is given by,

$$\begin{aligned} |g(R)\rangle &= \cos(\theta(R)/2) |\text{trans}\rangle + \sin(\theta(R)/2) |\text{cis}\rangle \\ |e(R)\rangle &= -\sin(\theta(R)/2) |\text{trans}\rangle + \cos(\theta(R)/2) |\text{cis}\rangle \end{aligned} \quad (1)$$

where $|e(R)\rangle$ and $|g(R)\rangle$ are the R -dependent adiabatic excited and ground state respectively. $|\text{trans}\rangle$ and $|\text{cis}\rangle$ are the (R -independent) crude diabatic electronic states

that describe the localized chemical character of each of the isomers. The ground-state PES has a predominant trans (cis) character to the left (right) of the barrier ($\theta(0) = 0$, $\theta(\pi) = \pi$) in Fig. 1a.

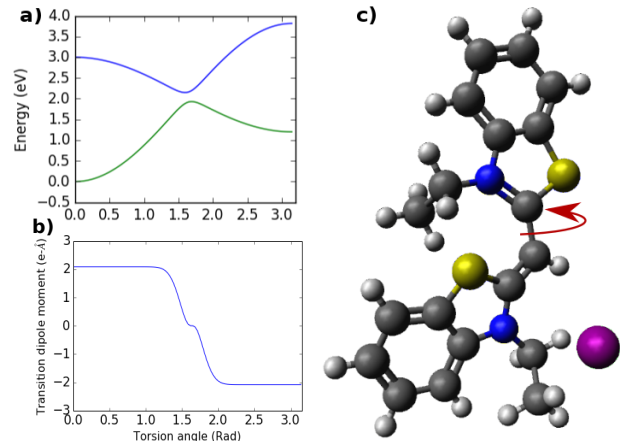


FIG. 1. a) Adiabatic potential energy surfaces (PESs) of the ground and first excited electronic states of the thiocyanine-like model molecule. b) Transition dipole moment ($\mu(R)$) of the model molecule in the adiabatic basis. c) Thiocyanine molecule. There exist two geometrical isomers of the molecule, a cis- and a trans-like configuration. The cis-trans isomerization of thiocyanine-like molecules occurs via a photo-induced torsion along the bridge which connects the aromatic rings.

Our USC model consists of a setup where an orthorhombic ensemble of thiocyanine molecules is placed on top of a thin spacer which, in turn, is on top of a metallic surface that hosts surface plasmons (SPs) [38] (see Fig. 2). The coupling between molecular electronic transitions and plasmons in the metal give rise to polaritons that are often called plexcitons [38, 39]. The ensemble is comprised of N_z single-molecule layers. The location of each molecule can be defined by the Cartesian coordinates $\mathbf{n} + (0, 0, z_s)$ where $\mathbf{n} = (\Delta_x n_x, \Delta_y n_y, 0)$ and $z_s = z_0 + \Delta_z s$ for the s -th layer. Here, the spacing between molecules along the i -th direction is denoted by Δ_i , and z_0 is the width of the spacer (see Fig. 2). We chose a SP electromagnetic environment because its evanescent intensity decreases fast enough with momentum \mathbf{k} (giving rise to vanishing light-matter coupling for large $|\mathbf{k}|$), resulting on a convergent Lamb-shift of the molecular ground-state. As shall be explained below, this circumvents technical complications of introducing renormalization cutoffs, as would be needed for a dielectric microcavity [28]. The Hamiltonian of the plexciton setup is given by $H = H_{el} + T_{nuc}$, where $T_{nuc} = \sum_i \frac{\mathbf{P}_i^2}{2M_i}$ is the nuclear kinetic energy operator and

$$\begin{aligned}
H_{el}(\mathbf{R}) = & \sum_{\mathbf{k}} \hbar\omega_{\mathbf{k}} a_{\mathbf{k}}^{\dagger} a_{\mathbf{k}} + \sum_{\mathbf{n},s} (\hbar\omega_e(R_{\mathbf{n},s}) - \hbar\omega_g(R_{\mathbf{n},s})) b_{\mathbf{n},s}^{\dagger}(R_{\mathbf{n},s}) b_{\mathbf{n},s}(R_{\mathbf{n},s}) \\
& + \sum_{\mathbf{k}} \sum_{\mathbf{n},s} g_{\mathbf{k}}^{\mathbf{n},s}(R_{\mathbf{n},s}) \left(a_{\mathbf{k}}^{\dagger} b_{\mathbf{n},s}(R_{\mathbf{n},s}) + a_{\mathbf{k}} b_{\mathbf{n},s}^{\dagger}(R_{\mathbf{n},s}) + a_{\mathbf{k}} b_{\mathbf{n},s}(R_{\mathbf{n},s}) + a_{\mathbf{k}}^{\dagger} b_{\mathbf{n},s}^{\dagger}(R_{\mathbf{n},s}) \right) \\
& + \sum_{\mathbf{n},s} \hbar\omega_g(R_{\mathbf{n},s}),
\end{aligned} \tag{2}$$

corresponds to the Dicke Hamiltonian [40]. Here $a_{\mathbf{k}}^{\dagger}$ ($a_{\mathbf{k}}$) is the creation (annihilation) operator for the SP mode with in-plane momentum \mathbf{k} which satisfies $[a_{\mathbf{k}}, a_{\mathbf{k}'}^{\dagger}] = \delta_{\mathbf{k},\mathbf{k}'}$, and $\mathbf{R} = \{R_{\mathbf{n}s}\}$ is an N -dimensional vector that describes the vibrational coordinates of the $N = N_x N_y N_z$ molecules of the ensemble, where N_i is the number of molecules along each ensemble axis. $\hbar\omega_g(R_{\mathbf{n},s})$ accounts for the ground-state energy of the molecule whose location in the ensemble is defined by \mathbf{n} and s . We introduce the (adiabatic R -dependent) exciton operator $b_{\mathbf{n},s}^{\dagger}(R_{\mathbf{n},s})$ ($b_{\mathbf{n},s}(R_{\mathbf{n},s})$) to label the creation (annihilation) of a Frenkel exciton (electronic excitation) with an energy gap $\hbar\omega_e(R_{\mathbf{n},s}) - \hbar\omega_g(R_{\mathbf{n},s})$ on the molecule located at $\mathbf{n} + z_s \hat{\mathbf{z}}$. The coefficients $\hbar\omega_{\mathbf{k}}$ and $g_{\mathbf{k}}^{\mathbf{n},s}(R_{\mathbf{n},s})$ stand for the energy of a SP with in-plane momentum \mathbf{k} and the coupling of the molecule located at $\mathbf{n} + z_s \hat{\mathbf{z}}$ with the latter, respectively. The dipolar SP-matter interaction is described by $g_{\mathbf{k}}^{\mathbf{n},s}(R_{\mathbf{n},s}) = h_{\mathbf{k}}(R_{\mathbf{n},s}) f_{\mathbf{k}}(z_s)$, where $h_{\mathbf{k}}(R_{\mathbf{n},s}) = -\boldsymbol{\mu}_{\mathbf{n},s}(R_{\mathbf{n},s}) \cdot \mathbf{E}_{\mathbf{k}}(\mathbf{n})$ is the projection of the molecular transition dipole $\boldsymbol{\mu}_{\mathbf{n},s}(R_{\mathbf{n},s})$ onto the in-plane component of the SP electric field $\mathbf{E}_{\mathbf{k}}(\mathbf{n})$ and $f_{\mathbf{k}}(z_s) = e^{-\alpha_{\mathbf{k}} z_s}$ is the evanescent field profile along the z direction, with $\alpha_{\mathbf{k}}$ being the decay constant in the molecular region ($z > 0$). The quantized plasmonic field $\hat{\mathbf{E}}_{\mathbf{k}} f_{\mathbf{k}}(z_s)$ has been discussed in previous works [38, 39, 41, 42] and reads $\hat{\mathbf{E}}_{\mathbf{k}}(\mathbf{n}) f_{\mathbf{k}}(z_s) = \sqrt{\frac{\hbar\omega_{\mathbf{k}}}{2\epsilon_0 S L_{\mathbf{k}}}} a_{\mathbf{k}} \hat{\chi}_{\mathbf{k}} e^{i\mathbf{k} \cdot \mathbf{n}} e^{-\alpha_{\mathbf{k}} z} + h.c.$, where ϵ_0 is the free-space permittivity, S is the coherence area of the plexciton setup, $L_{\mathbf{k}}$ is the quantization length, and $\hat{\chi}_{\mathbf{k}} = \hat{\mathbf{k}} + i \frac{|\mathbf{k}|}{\alpha_{\mathbf{k}}} \hat{\mathbf{z}}$ is the polarization. Note that the parametric dependence of the exciton operators on $R_{\mathbf{n},s}$ yield residual non-adiabatic processes induced by nuclear kinetic energy that may be relevant to the isomerization in question. We also highlight the fact that Eq. (2) includes both rotating (“energy conserving”) terms ($a_{\mathbf{k}}^{\dagger} b_{\mathbf{n},s}$ and $a_{\mathbf{k}} b_{\mathbf{n},s}^{\dagger}$) where a photon creation (annihilation) involves the concomitant annihilation (creation) of an exciton; and counterrotating (“non-energy conserving”) terms ($a_{\mathbf{k}} b_{\mathbf{n},s}$ and $a_{\mathbf{k}}^{\dagger} b_{\mathbf{n},s}^{\dagger}$) where there is a simultaneous annihilation (creation) of photon and exciton. These latter terms are ignored in the widely used Rotating Wave Approximation (RWA)[?], where light-matter coupling is weak compared to the transition energy. Since we are interested in

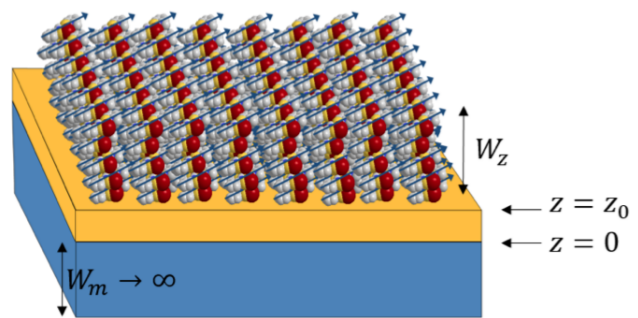


FIG. 2. *Plexciton setup.* The model consists of a surface-plasmon (SP) metal layer whose width W_m can be considered infinite in comparison with the relevant length scales of the structure. The thiacyanine molecular ensemble is separated from the metallic surface by a spacer of width z_0 ; the balls and sticks represent the molecules, while the arrows denote their transition dipole moments. The molecular layer has a height W_z and is extended along the x and y planes.

the USC, we shall keep them throughout.

III. METHODS

For simplicity, we assume that all the transition dipoles are equivalent and aligned along x , $\boldsymbol{\mu}_{\mathbf{n},s}(R_{\mathbf{n},s}) = \boldsymbol{\mu}(R_{\mathbf{n},s}) = \mu(R_{\mathbf{n},s}) \hat{\mathbf{x}}$; a departure of this perfect crystal condition does not affect the conclusions of this article. Furthermore, it is convenient to first restrict ourselves to the cases where all nuclei are fixed at the same configuration ($\mathbf{R} = \hat{\mathbf{R}}$, which denotes $R_{\mathbf{n},s} = R$ for all \mathbf{n} and s), so that we can take advantage of the underlying translational symmetry to introduce a delocalized exciton basis where the in-plane momentum \mathbf{k} is a good quantum number. The creation operator of this delocalized state is defined by $b_{\mathbf{k}}^{\dagger}(R) = \frac{1}{\sqrt{\mathcal{N}_{\mathbf{k}}(R)}} \sum_{\mathbf{n}} \sum_s f_{\mathbf{k}}(z_s) h_{\mathbf{k}}(R) b_{\mathbf{n},s}^{\dagger}(R)$, and the normalization squared is given by $\mathcal{N}_{\mathbf{k}}(R) = \sum_{\mathbf{n}} \sum_s |h_{\mathbf{k}}(R)|^2 |f_{\mathbf{k}}(z_s)|^2$ which, in the continuum limit, can be seen to be proportional to ρ , the number density of the molecular ensemble. In this collective basis, the

previously introduced $H_{el}(\mathbf{R})$ reads

$$\begin{aligned}
H_{el}(\tilde{\mathbf{R}}) &= \sum_{\mathbf{k}} \hbar\Delta(R)b_{\mathbf{k}}^{\dagger}(R)b_{\mathbf{k}}(R) + \sum_{\mathbf{k}} \hbar\omega_{\mathbf{k}}a_{\mathbf{k}}^{\dagger}a_{\mathbf{k}} \\
&+ \sum_{\mathbf{k}} \sqrt{\mathcal{N}_{\mathbf{k}}(R)} \left(a_{\mathbf{k}}^{\dagger}b_{\mathbf{k}}(R) + a_{\mathbf{k}}b_{\mathbf{k}}^{\dagger}(R) + a_{\mathbf{k}}b_{-\mathbf{k}}(R) + a_{\mathbf{k}}^{\dagger}b_{-\mathbf{k}}^{\dagger}(R) \right) + \sum_{\mathbf{k}} H_{\text{dark},\mathbf{k}}(R) + \sum_{\mathbf{k}} H_{\text{unklapp},\mathbf{k}}(R) + N\hbar\omega_g(R) \\
&= \sum_{\mathbf{k}} H_{\mathbf{k}}(R) + \sum_{\mathbf{k}} H_{\text{dark},\mathbf{k}}(R) + \sum_{\mathbf{k}} H_{\text{unklapp},\mathbf{k}}(R) + N\hbar\omega_g(R),
\end{aligned} \tag{3}$$

where $\Delta(R) = \omega_e(R) - \omega_g(R)$ is the exciton transition frequency.

$$H_{\text{dark},\mathbf{k}}(R) = \hbar\Delta(R)\mathbf{P}_{\text{dark},\mathbf{k}}(R) \tag{4}$$

accounts for the energy of the $(N_z - 1)$ -degenerate exciton states with in-plane momentum \mathbf{k} that do not couple to SPs, and are usually known as *dark states*. The latter are orthogonal to the bright exciton $b_{\mathbf{k}}^{\dagger}(R)|G_m(\tilde{\mathbf{R}})\rangle$ that couples to the SP field, where $|G_m(\tilde{\mathbf{R}})\rangle$ is the bare molecular ground-state ($b_{\mathbf{k}}(R)|G_m(\tilde{\mathbf{R}})\rangle = 0$). More specifically, $\mathbf{P}_{\text{dark},\mathbf{k}}(R) = \mathbf{I}_{\text{exc},\mathbf{k}}(R) - b_{\mathbf{k}}^{\dagger}(R)b_{\mathbf{k}}(R)$ is a projector operator onto the \mathbf{k} -th dark-state subspace, with $\mathbf{I}_{\text{exc}}(R) = \sum_{\mathbf{n},s} b_{\mathbf{n},s}^{\dagger}(R)b_{\mathbf{n},s}(R) = \sum_{\mathbf{k},s} b_{\mathbf{k},s}^{\dagger}(R)b_{\mathbf{k},s}(R) = \sum_{\mathbf{k}} \mathbf{I}_{\text{exc},\mathbf{k}}(R)$ being the identity on the exciton space, and $b_{\mathbf{k},s}^{\dagger}(R) = \frac{1}{\sqrt{N_x N_y}} \sum_{\mathbf{n}} e^{-i\mathbf{k}\cdot\mathbf{n}} b_{\mathbf{n},s}^{\dagger}(R)$. Finally,

$$\begin{aligned}
H_{\text{unklapp},\mathbf{k}}(R) &= \sum_{\mathbf{q}=\left(\frac{2\pi q_x}{\Delta x}, \frac{2\pi q_y}{\Delta y}\right)} \sqrt{\mathcal{N}_{\mathbf{k}}(R)} \left(a_{\mathbf{k}+\mathbf{q}}^{\dagger} b_{\mathbf{k}}(R) \right. \\
&\quad \left. + a_{\mathbf{k}+\mathbf{q}}^{\dagger} b_{-\mathbf{k}}^{\dagger}(R) + h.c. \right)
\end{aligned} \tag{5}$$

stands for the coupling of excitons with momentum \mathbf{k} to SP modes with momentum beyond the first excitonic Brillouin zone. $H_{\text{unklapp},\mathbf{k}}(R)$ is usually ignored given the large off-resonance between the SP energy and the exciton states; however, since this work pertains off-resonant effects, we considered it to acquire converged quantities in the calculations explained below. We also note that the normalization constant $\sqrt{\mathcal{N}_{\mathbf{k}}(R)}$ in Eq. 3 is precisely the collective SP-exciton coupling. As mentioned in the introduction, the condition $\sqrt{\mathcal{N}_{\mathbf{k}}(R)}/\hbar\Delta(R) > 0.1$ is often used to define the onset of USC [29], and it is fulfilled with the maximal density considered in our model (see Fig. 3) taking into account that the largest $\hbar\Delta(R)$ is 3 eV (See Fig. 1a). We note, as will be evident later, that our main results do not vary significantly by considering ratios $\sqrt{\mathcal{N}_{\mathbf{k}}(R)}/\hbar\Delta(R)$ below the aforementioned threshold.

A Bogoliubov transformation [33] permits the diagonalization of the Bloch Hamiltonian $H_{\mathbf{k}}$ in Eq. 3 by in-

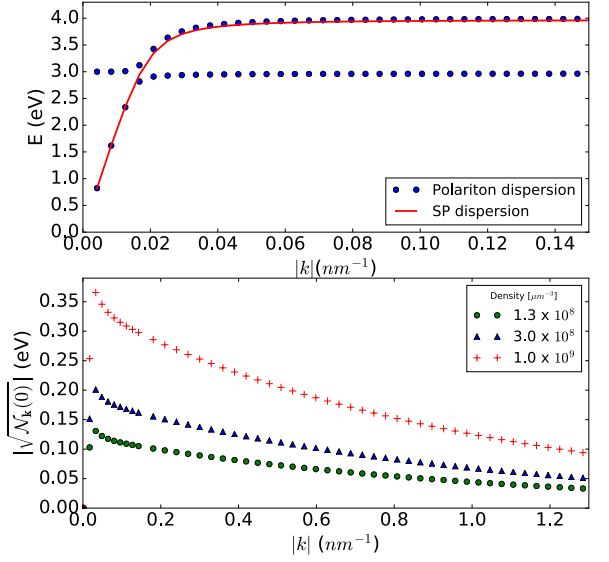


FIG. 3. *Upper*: Polariton dispersion that results from the interaction of a molecular ensemble with the plasmonic field; we chose $\rho = 1.0 \times 10^9 \mu\text{m}^{-3}$. *Lower*: Collective SP-exciton coupling at equilibrium geometry $\sqrt{\mathcal{N}_{\mathbf{k}}(0)}$ as a function of $|\mathbf{k}|$, assuming $\mu(R=0)$ and \mathbf{k} are parallel to the x axis. We consider a slab with $W_z = 120$ nm and compute couplings as a function of varying molecular densities ρ . The range of the resulting couplings is well above the plasmonic linewidth of the order of 10 meV [39], indicating the polaritonic onset of strong and ultrastrong light-matter coupling.

roducing the polariton quasiparticle operators

$$\xi_{\mathbf{k}}^j(R) = \alpha_{\mathbf{k}}^j a_{\mathbf{k}} + \beta_{\mathbf{k}}^j b_{\mathbf{k}}(R) + \gamma_{\mathbf{k}}^j a_{-\mathbf{k}}^{\dagger} + \delta_{\mathbf{k}}^j b_{-\mathbf{k}}^{\dagger}(R), \tag{6}$$

where $j = U, L$ and U (L) stands for the upper (lower) Bogoliubov polariton state. Notice that this canonical transformation is valid for a sufficiently large number of molecules N , where the collective exciton operators $b_{\mathbf{k}}(R)$, $b_{\mathbf{k}}^{\dagger}(R)$ are well approximated by bosonic operators [43].

The bare molecular ground-state with no photons in the absence of light-matter coupling $|G_m(\tilde{\mathbf{R}}); 0\rangle$, $(a_{\mathbf{k}}|G_m(\tilde{\mathbf{R}}); 0\rangle = b_{\mathbf{k}}(R)|G_m(\tilde{\mathbf{R}}); 0\rangle = 0$ for all \mathbf{k}) has a total extensive energy with molecular contributions only

$\langle G_m(\tilde{\mathbf{R}}); 0 | H_{el}(\tilde{\mathbf{R}}) | G_m(\tilde{\mathbf{R}}); 0 \rangle = N\hbar\omega_g(R)$. Upon inclusion of the counterrotating terms, the ground-state becomes the dressed Bogoliubov vacuum $|G(\tilde{\mathbf{R}})\rangle_d$, characterized by $\xi_{\mathbf{k}}^j(R) |G(\tilde{\mathbf{R}})\rangle_d = 0$ for all \mathbf{k} and j , with total energy ${}_d\langle G(\tilde{\mathbf{R}}) | H_{el}(\tilde{\mathbf{R}}) | G(\tilde{\mathbf{R}})\rangle_d = E_0(\tilde{\mathbf{R}})$, where the zero-point energy is given by

$$E_0(\tilde{\mathbf{R}}) = N\hbar\omega_g(R) + \frac{1}{2} \sum_{\mathbf{k}} \left(\sum_{j=U,L} \hbar\omega_{j,\mathbf{k}}(R) - \hbar\omega_{\mathbf{k}} - \hbar\Delta(R) \right), \quad (7)$$

$\{\hbar\omega_{j,\mathbf{k}}(R)\}$ being the eigenvalues of the Bogoliubov polariton branches given by

$$\omega_{L,U,\mathbf{k}}(R) = \sqrt{\frac{(\Delta(R))^2 + \omega_{\mathbf{k}}^2 \pm \sqrt{B(R)^2 + 16N_{\mathbf{k}}^2(R)\Delta(R)\omega_{\mathbf{k}}}}{2}}, \quad (8)$$

where we have introduced $B(R) = \omega_{\mathbf{k}}^2 - \Delta(R)^2$. A hallmark of the SC and USC regimes is the anticrossing splitting of the polariton energies at the \mathbf{k} value where the bare excitations are in resonance, $\Delta(R) = \omega_{\mathbf{k}}$ [42] (see Fig. 3). The sum in Eq. 7 accounts for the energy shift from the bare molecular energy $N\hbar\omega_g(R)$ due to interaction with the infinite number of SP modes in the setup. Using Eq. (8), it is illustrative to check that this shift vanishes identically when the non-RWA terms are ignored.

It is worth describing some of the physical aspects of the Bogoliubov ground-state $|G(\tilde{\mathbf{R}})\rangle_d$. With the numerically computed wavefunctions, we can use the inverse transformation of Eq. 6 to explicitly evaluate its SP and exciton populations [33],

$$n_{\mathbf{k}}^{SP} = {}_d\langle G(\tilde{\mathbf{R}}) | a_{\mathbf{k}}^\dagger a_{\mathbf{k}} | G(\tilde{\mathbf{R}})\rangle_d = \sum_j |\gamma_{\mathbf{k}}^j|^2, \quad (9a)$$

$$n_{\mathbf{k}}^{exc} = {}_d\langle G(\tilde{\mathbf{R}}) | b_{\mathbf{k}}^\dagger b_{\mathbf{k}} | G(\tilde{\mathbf{R}})\rangle_d = \sum_j |\delta_{\mathbf{k}}^j|^2, \quad (9b)$$

which give rise to humble $O(10^{-3})$ values per mode \mathbf{k} , considering a molecular ensemble with $\rho = 3 \times 10^8 \mu\text{m}^{-3}$ and $W_z = 120$ nm; this calculation is carried out using $N = 8 \times 10^7$, although results are largely insensitive to this parameter as long as it is sufficiently

large to capture the thermodynamic limit. The consequences of the dressing partially accounted for by Eq. (9) (partially since there are also correlations of the form ${}_d\langle G(\tilde{\mathbf{R}}) | b_{\mathbf{k}} a_{-\mathbf{k}} | G(\tilde{\mathbf{R}})\rangle_d$) are manifested as energetic effects on $|G_m(\tilde{\mathbf{R}}); 0\rangle$: $E_0(\tilde{\mathbf{R}}) - N\hbar\omega_g(R)$ can be interpreted as the energy stored in $|G(\tilde{\mathbf{R}})\rangle_d$ as a result of dressing; it is an extensive quantity of the ensemble, but becomes negligible when considering a per-molecule stabilization. For instance, in molecular ensembles with the aforementioned parameters we find $E_0(\tilde{\mathbf{0}}) - N\hbar\omega_g(0) = O(10^2)$ eV, which implies a $O(10^{-5})$ eV value per molecule; our calculations show that this intensive quantity is largely insensitive to total number of molecules. This observation raises the following questions: to what extent does photonic dressing would impact ground-state chemical reactivity? What are the relevant energy scales that dictate this impact? With these questions in mind, we aim to study the polaritonic effects on ground-state single-molecule isomerization events. To do so, we map out the PES cross section where we set one “free” molecule to undergo isomerization while fixing the rest at $R_{\mathbf{n},s} = 0$. A similar strategy has been used before in [24]. This cross section, described by $E_0(R_{\mathbf{n}_0,0}, 0, \dots, 0) \equiv E_0(R_{\mathbf{n}_0,0}, \tilde{\mathbf{0}}')$ ($R_{\mathbf{n}_0,0}$ being the coordinate of the unconstrained molecule), should give us an approximate understanding of reactivity starting from thermal equilibrium conditions, since the molecular configuration $\tilde{\mathbf{R}} = \tilde{\mathbf{0}}$ still corresponds to the global minimum of the modified ground-state PES, as will be argued later. By allowing one molecule to move differently than the rest, we weakly break translational symmetry. Rather than numerically implementing another Bogoliubov transformation, we can, to a very good approximation, account for this motion by treating the isomerization of the free molecule as a perturbation on $H_{el}(\tilde{\mathbf{0}})$. More precisely, we write $H_{el}(R_{\mathbf{n}_0,0}, \tilde{\mathbf{0}}') |G(R_{\mathbf{n}_0,0}, \tilde{\mathbf{0}}')\rangle_d = E_0(R_{\mathbf{n}_0,0}, \tilde{\mathbf{0}}') |G(R_{\mathbf{n}_0,0}, \tilde{\mathbf{0}}')\rangle_d$, where $H_{el}(R_{\mathbf{n}_0,0}, \tilde{\mathbf{0}}')$ is the sum of a translationally invariant piece $H_{el}(\tilde{\mathbf{0}})$ plus a perturbation due to the free molecule,

$$H_{el}(R_{\mathbf{n}_0,0}, \tilde{\mathbf{0}}') = H_{el}(\tilde{\mathbf{0}}) + V(R_{\mathbf{n}_0,0}). \quad (10)$$

The perturbation is explicitly given by

$$\begin{aligned} V(R_{\mathbf{n}_0,0}) &= H_{el}(R_{\mathbf{n}_0,0}, \tilde{\mathbf{0}}') - H_{el}(\tilde{\mathbf{0}}) \\ &= \hbar\Delta(R_{\mathbf{n}_0,0}) b_{\mathbf{n}_0,0}^\dagger(R_{\mathbf{n}_0,0}) b_{\mathbf{n}_0,0}(R_{\mathbf{n}_0,0}) - \hbar\Delta(0) b_{\mathbf{n}_0,0}^\dagger(0) b_{\mathbf{n}_0,0}(0) \\ &+ \sum_{\mathbf{k}} \left\{ g_{\mathbf{k}}^{\mathbf{n}_0,0}(R_{\mathbf{n}_0,0}) \left[b_{\mathbf{n}_0,0}(R_{\mathbf{n}_0,0}) + b_{\mathbf{n}_0,0}^\dagger(R_{\mathbf{n}_0,0}) \right] - g_{\mathbf{k}}^{\mathbf{n}_0,0}(0) \left[b_{\mathbf{n}_0,0}(0) + b_{\mathbf{n}_0,0}^\dagger(0) \right] \right\} \left[a_{\mathbf{k}} + a_{\mathbf{k}}^\dagger \right] \\ &+ \hbar\omega_g(R_{\mathbf{n}_0,0}) - \hbar\omega_g(0). \end{aligned} \quad (11)$$

Notice that we have chosen the free molecule to be located at an arbitrary in-plane location \mathbf{n}_0 and at the very bottom of the slab at $s = 0$, where light-matter coupling is strongest as a result of the evanescent field profile along the z direction. We write an expansion of the PES cross section as $E_0(R_{\mathbf{n}_0,0}, \tilde{\mathbf{O}}') = \sum_{q=0}^{\infty} E_0^{(q)}(R_{\mathbf{n}_0,0}, \tilde{\mathbf{O}}')$, where q labels the $O(V^q)$ perturbation correction. The zeroth order term is the Bogoliubov vacuum energy associated to every molecule being at the equilibrium geometry $E_0^{(0)}(R_{\mathbf{n}_0,0}, \tilde{\mathbf{O}}') = E_0(\tilde{\mathbf{O}})$ as in Eq. (7). The $O(V)$ correction corresponds to $\hbar\omega_g(R_{\mathbf{n}_0,0}) - \hbar\omega_g(0)$, merely describing the PES of the isomerization of the bare molecule in the absence of coupling to the SP field. The contribution of the SP field on the PES cross-section of interest appears at $O(V^2)$, and it is given by

$$E^{(2)}(R_{\mathbf{n}_0,0}, \tilde{\mathbf{O}}') \approx \sum_{\substack{\mathbf{k}_1 \leq \mathbf{k}_2 \\ i,j=UP,LP}} \frac{|\langle \mathbf{k}_1, i; \mathbf{k}_2, j | V(R_{\mathbf{n}_0,0}) | G(\tilde{\mathbf{O}}) \rangle_d|^2}{E_0(\tilde{\mathbf{O}}) - E_{\mathbf{k}_1, \mathbf{k}_2, i, j}^{(0)}}, \quad (12)$$

$$\begin{aligned} \langle \mathbf{k}_1, i; \mathbf{k}_2, j | V(R_{\mathbf{n}_0,0}) | G(\tilde{\mathbf{O}}) \rangle_d &= F^{\mathbf{k}_2}(R_{\mathbf{n}_0,0}) D_{\mathbf{k}_1} \left(-\delta_{-\mathbf{k}_1}^i \alpha_{\mathbf{k}_2}^j + \delta_{-\mathbf{k}_1}^i \gamma_{-\mathbf{k}_2}^j - \beta_{\mathbf{k}_1}^i \gamma_{-\mathbf{k}_2}^j + \beta_{\mathbf{k}_1}^i \alpha_{\mathbf{k}_2}^j \right) \\ &+ F^{\mathbf{k}_1}(R_{\mathbf{n}_0,0}) D_{\mathbf{k}_2} \left(-\delta_{-\mathbf{k}_2}^j \alpha_{\mathbf{k}_1}^i + \delta_{-\mathbf{k}_2}^j \gamma_{-\mathbf{k}_1}^i - \beta_{\mathbf{k}_2}^j \gamma_{-\mathbf{k}_1}^i + \beta_{\mathbf{k}_2}^j \alpha_{\mathbf{k}_1}^i \right), \end{aligned} \quad (13)$$

where $F^{\mathbf{k}}(R) = \cos(\theta(R))g_{\mathbf{k}}^{\mathbf{n}_0,0}(R) - \cos(\theta(0))g_{\mathbf{k}}^{\mathbf{n}_0,0}(0)$ depends on the mixing angle that describes the change of character of $b_{\mathbf{n}_0,0}^{\dagger}(R)$ as a function of R (see Equation (1)); it emerges as a consequence of coupling molecular states at different configurations. $D_{\mathbf{k}} = \langle G_m(\tilde{\mathbf{R}}); 0 | b_{\mathbf{n}_0,0}(0) b_{\mathbf{k}}^{\dagger}(0) | G_m(\tilde{\mathbf{R}}); 0 \rangle = \frac{1}{\sqrt{N_x N_y}} \sqrt{\frac{1 - e^{-2\alpha_{\mathbf{k}} \Delta_z}}{1 - e^{-2\alpha_{\mathbf{k}} \Delta_z N_z}}}$ accounts for the weight of a localized exciton operator in a delocalized one, such as the participation of $b_{\mathbf{n}_0,0}^{\dagger}(0)$ in $b_{\mathbf{k}}^{\dagger}(0)$. Eq. (13) reveals that the maximal contribution of each double-polariton Bogoliubov state to the energetic shift of the considered PES cross section $E(R_{\mathbf{n}_0,0}, \tilde{\mathbf{O}}')$ is of the order of $\frac{g_{\mathbf{k}}^{\mathbf{n}_0,0}(0)}{\sqrt{N_x N_y}}$. Considering macroscopic molecular ensembles with large $N \approx 10^7$, we computed Eq. 12 by means of an integral approximation over the polariton modes \mathbf{k} .

where $|\mathbf{k}_1, i; \mathbf{k}_2, j\rangle \equiv \xi_{\mathbf{k}_1}^{i\dagger}(0) \xi_{\mathbf{k}_2}^{\dagger j}(0) | G(\tilde{\mathbf{O}}) \rangle_d$ and $E_{\mathbf{k}_1, \mathbf{k}_2, i, j}^{(0)} = \hbar(\omega_{i, \mathbf{k}_1}(0) + \omega_{j, \mathbf{k}_2}(0))$. As shown in the Appendix, the approximation in Eq. (12) consists of ignoring couplings between $|G(\tilde{\mathbf{O}})\rangle_d$ and states with three and four Bogoliubov polariton excitations, since their associated matrix elements become negligible in the thermodynamic limit compared to their double excitation counterparts. The remaining matrix elements can be calculated by expressing the operators $a_{\mathbf{k}}, a_{\mathbf{k}}^{\dagger}, b_{\mathbf{n}_0,0}, b_{\mathbf{n}_0,0}^{\dagger}$ in Eq. (11) in terms of the Bogoliubov operators $\xi_{\mathbf{k}}^j(0), \xi_{\mathbf{k}}^{\dagger j}(0)$ (see Eq. (6)), leading to

IV. RESULTS AND DISCUSSION

A. Energetic effects

We carry out our calculations with ρ in the range of 10^6 to 10^9 molecules μm^{-3} keeping $W_z = 120$ nm (see Fig. 4); to obtain results in the thermodynamic limit, our calculations take $N = 8 \times 10^7$, even though the exact value is unimportant as long as it is sufficiently large to give converged results. The results displayed in Fig. 4 show that the second order energy corrections to the isomerization PES $E^{(2)}(R_{\mathbf{n}_0,0}, \tilde{\mathbf{O}}')$, and in particular $E^{(2)}(R_{\mathbf{n}_0,0} = R^*, \tilde{\mathbf{O}}') \approx -0.25$ meV, are negligible in comparison with the bare activation barrier $E_a = \hbar\omega_g(R^*) - \hbar\omega_g(0) = \hbar\omega_g(R^*) \approx 1.8$ eV, where $R^* \approx 1.64$ rad corresponds to the transition state. From Fig. 1b, we notice that there is a substantial difference in SP-exciton coupling between the equilibrium ($R_{\mathbf{n}_0,0} = 0$) and transition state geometries ($R_{\mathbf{n}_0,0} = R^*$). Since the perturbation in Eq. (11) is defined with respect to the equilibrium geometry, $|E^{(2)}(R_{\mathbf{n}_0,0}, \tilde{\mathbf{O}}')|$ maximizes at the barrier geometry. To get some insight on the order of magnitude of the result, we note that the sum shown in Eq. 12 can be very roughly approximated as

$$\begin{aligned}
E^{(2)}(R_{\mathbf{n}_0,0}, \tilde{\mathbf{0}}') &= O \left[- \sum_{\mathbf{k}_1 \leq \mathbf{k}_2} \frac{[g_{\mathbf{k}_1}^{\mathbf{n}_0,0}(R_{\mathbf{n}_0,0})]^2 D_{\mathbf{k}_2}^2 + [g_{\mathbf{k}_2}^{\mathbf{n}_0,0}(R_{\mathbf{n}_0,0})]^2 D_{\mathbf{k}_1}^2}{(\hbar\omega_{\mathbf{k}_1} + \hbar\omega_{\mathbf{k}_2})/2 + \hbar\omega_e(R_{\mathbf{n}_0,0})} \right] \\
&= O \left[- \frac{1}{N_x N_y} \sum_{\mathbf{k}_1 \leq \mathbf{k}_2} \frac{[g_{\mathbf{k}_1}^{\mathbf{n}_0,0}(R_{\mathbf{n}_0,0})]^2 + [g_{\mathbf{k}_2}^{\mathbf{n}_0,0}(R_{\mathbf{n}_0,0})]^2}{(\hbar\omega_{\mathbf{k}_1} + \hbar\omega_{\mathbf{k}_2})/2 + \hbar\omega_e(R_{\mathbf{n}_0,0})} \right] \\
&= O \left[- \sum_{\mathbf{k}} \frac{[g_{\mathbf{k}}^{\mathbf{n}_0,0}(R_{\mathbf{n}_0,0})]^2}{\hbar\omega_{\mathbf{k}} + \hbar\omega_e(R_{\mathbf{n}_0,0})} \right] \\
&= O(E_{LS}(R_{\mathbf{n}_0,0})).
\end{aligned} \tag{14}$$

In the first line, we used the fact that $\langle \mathbf{k}_1, i; \mathbf{k}_2, j | V(R_{\mathbf{n}_0,0}) | G(\tilde{\mathbf{0}}) \rangle_d \approx [g_{\mathbf{k}_1}^{\mathbf{n}_0,0}(R_{\mathbf{n}_0,0})]^2 D_{\mathbf{k}_2}^2 + [g_{\mathbf{k}_2}^{\mathbf{n}_0,0}(R_{\mathbf{n}_0,0})]^2 D_{\mathbf{k}_1}^2$ and averaged the Bogoliubov polariton excitation energies. In the second line, assuming that the $\mathbf{k} \gg 0$ values contribute the most, we have $D_{\mathbf{k}} \approx \frac{1}{\sqrt{N_x N_y}}$. Finally, in the third line, we have used the fact that the sum of terms over $\mathbf{k}_1, \mathbf{k}_2$ is roughly equal to $N_x N_y$ times a single sum over \mathbf{k} of terms of the same order. The reason why we are interested in the final approximation is because it corresponds to the Lamb shift of a single isolated molecule, which can be calculated to be $E_{LS}(0) = 0.16$ meV. Typically, Lamb shift calculations require a cutoff to avoid unphysical divergences [44]; we stress that in our plexciton model, this is not necessary due to the decaying $|g_{\mathbf{k}}^{\mathbf{n}_0,0}(R_{\mathbf{n}_0,0})|$ as a function of $|\mathbf{k}|$. The fact that the corrections $E^{(2)}(R_{\mathbf{n}_0,0}, \tilde{\mathbf{0}}')$ have a similar order of magnitude to single-molecule Lamb shifts give a pessimistic conclusion of harnessing USC to control ground-state chemical reactions. Note, however, from calculations in Fig. 4, that there is variability in $E^{(2)}(R_{\mathbf{n}_0,0}, \tilde{\mathbf{0}}')$ as a function of molecular density (since density alters the character of the Bogoliubov polaritons), although the resulting values are always close to $E_{LS}(0)$. The molecular density cannot increase without bound, since there exists a minimum molecular contact distance determined by a van der Waals radius of the order of 0.3 nm for organic molecules [45], giving a maximum density of $\rho \approx 10^{10}$ molecules/ μm^3 .

The results discussed so far describe the energy profile of the isomerization of a single molecule keeping the rest at equilibrium geometry. It is intriguing to inquire the effects of the SP field in a concerted isomerization of two or more molecules, while keeping the rest fixed at equilibrium geometry. Generalizing Eqs. (11)–(13) to a two-molecule perturbation $V(R_{\mathbf{n}_0,0}, R_{\mathbf{n}_1,0})$, we computed the second order energetic corrections to the 2D-PES that describe the isomerization of two neighbouring molecules at \mathbf{n}_0 and at $\mathbf{n}_1 \equiv \mathbf{n}_0 + \Delta_x \hat{\mathbf{x}}$, keeping the other molecules fixed at $R_{\mathbf{n},s} = 0$. The results are reported in

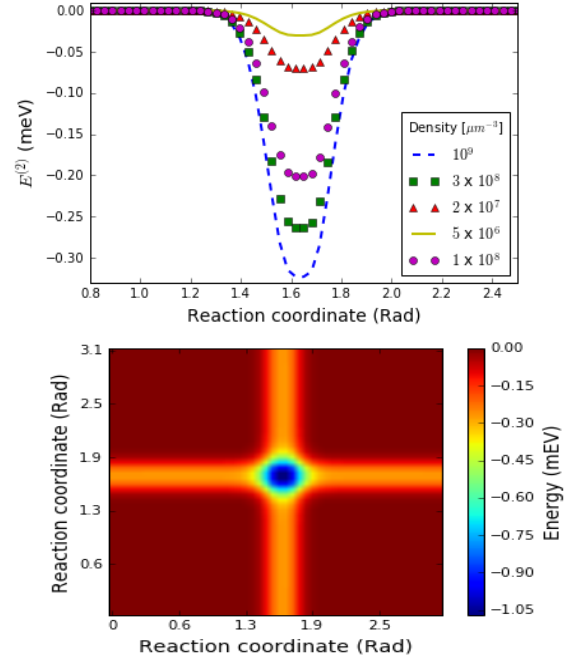


FIG. 4. *Upper*: Second order energy correction $E^{(2)}(R_{\mathbf{n}_0,0}, \tilde{\mathbf{0}}')$ of PES for one molecule isomerizing along the torsional coordinate $R_{\mathbf{n}_0,0}$; the rest of the molecules are fixed at the equilibrium geometry. Calculations are displayed for various densities ρ , keeping $W_z = 120$ nm. Energy corrections are due to SP-exciton (see Eq. 12). Note also that the energy scale of this correction is negligible in comparison with the energy barrier of the reaction (see Fig. 1a). *Lower*: Same plot as in left, but for the 2D-ground-isomerization PES of two molecules, keeping the configuration of the other molecules at equilibrium ($E^{(2)}(R_0, R_1, \tilde{\mathbf{0}}')$); the density $\rho = 3 \times 10^8$ molecules/ μm^3 .

Fig. 4 for $\rho = 3 \times 10^8$ molecules/ μm^3 , although outcomes of the same order of magnitude are obtained for the other densities considered in the one-dimensional case. The two-dimensional PES cross-section $E^{(2)}(R_{\mathbf{n}_0,0}, R_{\mathbf{n}_1,0}, 0, \dots, 0) \equiv E^{(2)}(R_{\mathbf{n}_0,0}, R_{\mathbf{n}_1,0}, \tilde{\mathbf{0}}')$ shows the existence of an energetic enhancement for

the concerted isomerization with respect to two independent isomerizations, *i.e.* $E^{(2)}(R_{\mathbf{n}_0,0} = R^*, R_{\mathbf{n}_1,0} = R^*, \tilde{\mathbf{O}}') \approx 4E^{(2)}(R_{\mathbf{n}_0,0} = R^*, \tilde{\mathbf{O}}')$. This enhancement is due to a constructive interference arising at the amplitude level, $\langle \mathbf{k}_1, i; \mathbf{k}_2, j | V(R_{\mathbf{n}_0,0} = R^*, R_{\mathbf{n}_1,0} = R^*) | G(\tilde{\mathbf{O}}) \rangle_d \approx 2 \langle \mathbf{k}_1, i; \mathbf{k}_2, j | V(R_{\mathbf{n}_0,0} = R^*) | G(\tilde{\mathbf{O}}) \rangle_d$ for values of $\mathbf{k}_1, \mathbf{k}_2 \ll \frac{1}{\Delta_x}$, such that the phase difference between the isomerizing molecules is negligible. Interestingly, choosing the neighbouring molecules along the x direction is important for this argument; if instead we consider neighbours along z (molecular positions \mathbf{n}_0 and $\mathbf{n}_0 + \Delta_z \hat{z}$), these interferences vanish and we approximately get the independent molecules result $E^{(2)}(R_{\mathbf{n}_0,0} = R^*, R_{\mathbf{n}_0,1} = R^*, \tilde{\mathbf{O}}') \approx 2E^{(2)}(R_{\mathbf{n}_0,0} = R^*, \tilde{\mathbf{O}}')$.

In light of the nontrivial energetic shift of the two-molecule case, it is pedagogical to consider the SP effects on the cross-section of the concerted isomerization of the whole ensemble, even though it is highly unlikely that this kinetic pathway will be of any relevance, especially considering the large barrier for the isomerization of each molecule. Notice that the conservation of translational symmetry in this scenario allows for the exact (nonperturbative) calculation of the energetic shift $E_0(\tilde{\mathbf{R}}) - N\hbar\omega_g(R)$ by means of Eq. 7. Our numerical calculations reveal an energetic stabilization profile, which is displayed in Fig. 5 for a molecular ensemble with $\rho = 3 \times 10^8$ molecules μm^{-3} . As expected, we observe a stabilization of reactant and product regions of the ground-state PES. This is a consequence of the transition dipole moment being the strongest at those regions, as opposed to the transition state, see Fig. 1b. However, even though these energetic effects are of the order of hundreds of eV, they are negligible in comparison with the total ground-state PES $N\hbar\omega_g(R)$, or more specifically, to the transition barrier $NE_a = N\hbar\omega_g(R^*)$ for the concerted reaction. Importantly, the change in activation energy per molecule in the concerted isomerization with respect to the bare case $|\Delta E_a| = \left| \left(\frac{E_0(\tilde{\mathbf{R}}^*) - E_0(\tilde{\mathbf{O}})}{N} - E_a \right) \right| \approx 0.009 \text{ meV}$ is more than one order of magnitude smaller than the corresponding quantity $|E^{(2)}(R_{\mathbf{n}_0,0} = R^*, \tilde{\mathbf{O}}')| \approx 0.25 \text{ meV}$ for the single-molecule isomerization case, see Fig. 4 and inset of Fig. 5. We believe that the reason for this trend is that the isomerization of n molecules, $n \ll N$, translates into a perturbation which breaks the original translational symmetry of the molecular ensemble. This symmetry breaking permits the interaction of the molecular vacuum with the polaritonic \mathbf{k} -state reservoir without a momentum-conservation restriction. This is reflected in Eq. 12, where the sum is carried out over two not necessarily equal momenta. In contrast, in the case of the concerted isomerization of N molecules, the translational symmetry of the system is preserved, which in turn restricts the coupling of the vacuum $|G(\tilde{\mathbf{O}})\rangle_d$ to

excited states with $\mathbf{k}_{\text{exc}} = -\mathbf{k}_{\text{phot}}$.

Another intriguing observation is that, for this concerted isomerization, the SP energetic effect per molecule $\frac{E_0(\tilde{\mathbf{R}})}{N}$ diminishes with the width of the slab W_z . This is the case given that the SP quantization length $L_{\mathbf{k}}$ decays quickly with $|\mathbf{k}|$ so that only the closest layers interact strongly with the field. When we divide the total energetic effects due to the SP modes by $N = N_x N_y N_z$, we obtain that $\frac{E_0(\tilde{\mathbf{R}})}{N} = O(\frac{1}{N_z})$ for large W_z . The energetic shifts in all the scenarios discussed above are negligible with respect to the corresponding energy barriers and the thermal energy scale at room temperature which, unfortunately, signal the irrelevance of USC to alter ground-state chemical reactivity for this isomerization model. Although there is an overall (extensive) stabilization of the molecular ensemble ground state, this effect is distributed across the ensemble, giving no possibility to alter the chemical reaction kinetics or thermodynamics considerably. However, we highlight the intriguing interferences observed in the concerted isomerization processes. Even though they will likely be irrelevant for this particular reaction, they might be important when dealing with reactions with very low barriers, especially when considering that these concerted pathways are combinatorially more likely to occur than the single-molecule events in the large N limit. This is intriguing in light of the study carried out in [46], which discusses a different but related effect of many reactions triggered by a single photon.

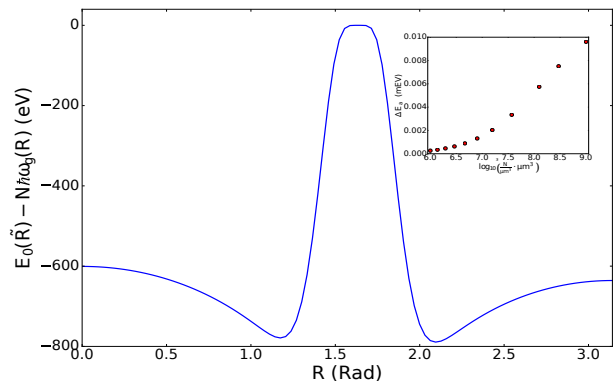


FIG. 5. *Main*: profile of the energy stabilization of the concerted isomerization ($E_0(\tilde{\mathbf{R}}) - N\hbar\omega_g(R)$, see Eq. 7) of the whole molecular ensemble discussed in the main text, due to the interaction with the plasmonic field. We consider a molecular macroscopic ensemble ($N = 8 \times 10^7$) with density $\rho = 3 \times 10^8$ molecules/ μm^3 . *Inset*: molecular-density dependence of the energy shift of the energy barrier per molecule $|\Delta E_a|$ (see main text) due to the plasmonic field, in this concerted scenario.

B. Effects on non-adiabatic dynamics

Finally, we discuss the importance of the nonadiabatic effects afforded by nuclear kinetic energy. Previous works have considered the nonadiabatic effects between polariton states at the level of SC [26, 47]. Alternatively, the consideration of nonadiabatic effects in USC for a single molecule in a cavity was provided in [48]; here, we address these issues for the many-molecule case and consider both polariton and dark state manifolds. One could expect significantly modified non-adiabatic dynamics about nuclear configurations where the transition dipole moment magnitude $|\mu_{\mathbf{n},s}(R_{\mathbf{n},s})|$ is large, given a reduction in the energy gap between the ground and the lower Bogoliubov polariton state. However, as we show below, this energetic effect is not substantial due to the presence of dark states.

We consider the magnitude of the non-adiabatic couplings (NACs) for the isomerization of a single molecule with reaction coordinate $R_{\mathbf{n}_0,0}$. For a region about $\tilde{\mathbf{R}} = \tilde{\mathbf{0}}$, we estimate the magnitude of the NAC between $|G(\tilde{\mathbf{0}})\rangle_d$ and a state $|\mathbf{k}, i\rangle = \xi_{\mathbf{k}}^{ii}(0)|G(\tilde{\mathbf{0}})\rangle_d$ as:

$$\begin{aligned} |A_{\mathbf{k},i;g}(0)| &= \left| \langle \mathbf{k}, i | \frac{\partial}{\partial R_{\mathbf{n}_0,0}} |G(\tilde{\mathbf{0}})\rangle_d \right| \\ &\approx \left| \beta_{\mathbf{k}}^i D_{\mathbf{k}} \left\langle e_{\mathbf{n}_0,0}(0) \left| \frac{\partial}{\partial R_{\mathbf{n}_0,0}} \right| g_{\mathbf{n}_0,0}(0) \right\rangle \right|, \end{aligned} \quad (15)$$

where $|g_{\mathbf{n}_0,0}(0)\rangle$ ($|e_{\mathbf{n}_0,0}(0)\rangle$) is the ground (excited) adiabatic state of the single molecule under consideration (see Eq. (1)) and we have ignored the derivatives of $\beta_{\mathbf{k}}^i$ and $D_{\mathbf{k}}$ with respect to $R_{\mathbf{n}_0,0}$, assuming they are small at $\tilde{\mathbf{R}} = \tilde{\mathbf{0}}$, where the chemical character of the Bogoliubov polariton states does not change significantly with respect to nuclear coordinate. This is a consequence of the slowly changing transition dipole moment of the model molecule around $R_{\mathbf{n}_0,0} = 0$, see Fig. 1b. Notice that we have also assumed $\langle \mathbf{k}, i | e_{\mathbf{n}_0,0}(0) \rangle \approx \beta_{\mathbf{k}}^i D_{\mathbf{k}}$, where we have used the fact that $\beta_{\mathbf{k}}^i \gg \gamma_{\mathbf{k}}^i$, thus ignoring counterrotating terms, which as we have seen, give negligible contributions. The time-evolution of a nuclear wavepacket in the ground-state will be influenced by the Bogoliubov polariton states, each of which will contribute with a finite probability of transition out of $|G(\tilde{\mathbf{0}})\rangle_d$. From semiclassical arguments [49], we can estimate the transition probability $|C_{\mathbf{k}}^i(0)|^2$ for a nuclear wavepacket on the ground-state PES at $\tilde{\mathbf{R}} = \mathbf{0}$ to the state $|\mathbf{k}, i\rangle$,

$$\begin{aligned} |C_{\mathbf{k}}^i(0)|^2 &\approx \left| \frac{\hbar v_{nuc} A_{\mathbf{k},i;g}(0)}{\hbar \omega_{i,\mathbf{k}}(0) - \hbar \omega_g(0)} \right|^2 \\ &= \left| \frac{\hbar v_{nuc} \beta_{\mathbf{k}}^i D_{\mathbf{k}}}{\hbar \omega_{i,\mathbf{k}}(0) - \hbar \omega_g(0)} \right|^2 \\ &\times \left| \left\langle e_{\mathbf{n}_0,0}(0) \left| \frac{\partial}{\partial R_{\mathbf{n}_0,0}} \right| g_{\mathbf{n}_0,0}(0) \right\rangle \right|^2, \end{aligned} \quad (16)$$

v_{nuc} being the expectation value of the nuclear velocity. However, the Bogoliubov polariton \mathbf{k} -states are only a small subset of the excited states of the problem. As mentioned right after Eq. 3, the plexciton setup contains $N_z - 1$ dark excitonic states for every \mathbf{k} (eigenstates of $H_{\text{dark},\mathbf{k}}(0)$, see discussion right after Eq. 3); we ignore the very off-resonant couplings considered in $H_{\text{unklapp},\mathbf{k}}(0)$. The dark states also couple to $|G(\tilde{\mathbf{0}})\rangle_d$ non-adiabatically, with the corresponding transition probability out of the ground state being,

$$\begin{aligned} |C_{\mathbf{k}}^{\text{dark}}(0)|^2 &\approx \sum_Q \left| \frac{\hbar v_{nuc} A_{\mathbf{k},Q;g}(0)}{\hbar \Delta(0)} \right|^2 \\ &\approx P_{bare}(0) \left(\frac{1}{N_x N_y} - |D_{\mathbf{k}}|^2 \right), \end{aligned} \quad (17)$$

Here, we have summed over all dark states Q for a given \mathbf{k} and used $P_{bare}(0) = \left| \frac{v_{nuc}}{\Delta(0)} \right|^2 \left| \left\langle e_{\mathbf{n}_0,0}(0) \left| \frac{\partial}{\partial R_{\mathbf{n}_0,0}} \right| g_{\mathbf{n}_0,0}(0) \right\rangle \right|^2$ to denote the probability of transition out of the ground state in the absence of coupling to the SP field. In Eq. (17) we used the fact that the projection $|e_{\mathbf{n}_0,0}(0)\rangle$ onto the dark \mathbf{k} manifold of exciton states is $|\mathbf{P}_{\text{dark},\mathbf{k}}(0)|e_{\mathbf{n}_0,0}(0)\rangle|^2 = \langle e_{\mathbf{n}_0,0}(0) | \mathbf{I}_{\text{exc},\mathbf{k}}(0) | e_{\mathbf{n}_0,0}(0) \rangle - |D_{\mathbf{k}}|^2 = \frac{1}{N_x N_y} - |D_{\mathbf{k}}|^2$, with $\mathbf{P}_{\text{dark},\mathbf{k}}(0)$ being the corresponding projector (see Eq. (4)). We noticed that when $|\mathbf{k}| \rightarrow 0$, the quantization volume $L_{\mathbf{k}}$ of the plasmonic field spans all the molecular-ensemble volume resulting in completely delocalized bright and dark exciton states across the different layers of the slab, $|\mathbf{P}_{\text{dark},\mathbf{k}}|e_{\mathbf{n}_0,0}(0)\rangle|^2 = \frac{N_z - 1}{N_x N_y}$, and the dark states give the major contribution to the nonadiabatic dynamics. On the other hand, when $|\mathbf{k}| \rightarrow \infty$, the plasmonic field interacts with the molecular layer at the bottom of the slab only and $|\mathbf{P}_{\text{dark},\mathbf{k}}|e_{\mathbf{n}_0,0}(0)\rangle|^2 \rightarrow 0$. The dark states do not participate, because the molecule located at \mathbf{n}_0 only overlaps with the bright state which is concentrated across the first layer of the slab (the dark states, being orthogonal to the bright one, are distributed in the upper layers, and do not overlap with $|e_{\mathbf{n}_0,0}\rangle$). With these results, we can compute the probability of transition out of the ground-state P_{out} as

$$P_{out}(0) = \sum_{\mathbf{k}} \left[\sum_i |C_{\mathbf{k}}^i(0)|^2 + |C_{\mathbf{k}}^{\text{dark}}(0)|^2 \right]. \quad (18)$$

In view of the large off-resonant nature of most SP modes with respect to $\hbar \Delta(0)$ (see Fig. 3) and Eq. (17), we have $\sum_i |C_{\mathbf{k}}^i(0)|^2 \approx P_{bare}(0) |D_{\mathbf{k}}|^2$, such that $P_{out}(0) \approx P_{bare}(0)$. In our model, this is the case, since the plexciton anticrossing occurs at small $|\mathbf{k}|$ and the SP energy quickly increases and reaches an asymptotic value after that point (see Fig. 3).

Using the parameters in [37], we obtain $\langle e(R_{\mathbf{n}_0,0}) | \frac{\partial}{\partial R_{\mathbf{n}_0,0}} | g(R_{\mathbf{n}_0,0}) \rangle \approx 0.01 \text{ \AA}^{-1}$, where we

have assumed an effective radius of 1 \AA for the isomerization mode of the model molecule. We get an estimate of $v_{nuc} \approx 1 \text{ \AA} \omega_{nuc} = 1 \text{ \AA} \sqrt{\frac{k_B T}{m}} = 9 \times 10^{10} \text{ \AA s}^{-1}$ using $k_B = 8.62 \times 10^{-5} \text{ eV K}^{-1}$, $T = 298 \text{ K}$ and $m = 2.5 \text{ amu } \text{ \AA}^2$. Finally, applying $\Delta(0) = 3 \text{ eV}$ gives $P_{bare}(0) \approx 10^{-7}$, which is a negligible quantity. A more pronounced polariton-effect is expected close to the PES avoided crossing. However, the rapid decay of the transition dipole moment in this region (see Fig. 1a) precludes the formation of polaritonic states that could have affected the corresponding nonadiabatic dynamics. To summarize this part, even when the USC effects on the nonadiabatic dynamics are negligible for our model, the previous discussion as well as Eq. (18) distill the design principle that controls these processes in other polariton systems: the plexciton anticrossings should happen at large \mathbf{k} values to preclude the overwhelming effects of the dark states. This principle will be explored in future work in other molecular systems.

The negligible polariton effect on the NACs, and the magnitude of the energetic effects on the electronic energy landscape are strong evidence to argue that the chemical yields and rates of the isomerization problem in question remain intact with respect to the bare molecular ensemble.

V. CONCLUSIONS

We showed in this work that, for the ground state landscape of a particular isomerization model, there is no relevant collective stabilization effect by USC to SPs which can significantly alter the kinetics or thermodynamics of the reaction, in contrast with previous calculations which show such possibilities in the Bogoliubov polariton landscapes [4, 24]. The negligible energetic corrections to the ground-state PES per molecule can be approximated and interpreted as Lamb shifts [44] experienced by the molecular states due to the interaction with off-resonant plasmonic modes. The key dimensionless parameter which determines the USC effect on the ground-state PES is the ratio of the individual coupling to the transition frequency $g_{\mathbf{k}}^{n,s}/\hbar\Delta$. This finding is similar to the conclusions of a recent work [26, 28]. In particular, it is shown in [28] that the rotational and vibrational degrees of freedom of molecules exhibit a self-adaptation which only depends on light-matter coupling at the single-molecule level. Therefore, more remarkable effects are expected in the regime of USC of a single molecule interacting with an electric field. To date, the largest single molecule interaction energy achievable experimentally is around 90 meV [27] in an ultralow nanostructure volume. This coupling strength is almost two orders of magnitude larger than those in our model. Also, previous works have shown [32, 50] that this regime is achievable for systems with

transition frequencies on the microwave range. Additionally, the experimental realization of vibrational USC has been carried out recently [36]. The latter also suggests the theoretical exploration of USC effects on chemical reactivity at the rotational or vibrational energy scales, where the energy spacing between levels is significantly lower than typical electronic energy gaps.

We highlighted some intriguing quantum-coherent effects where concerted reactions can feature energetic effects that are not incoherent combinations of the bare molecular processes. These interference effects are unlikely to play an important role in reactions exhibiting high barriers compared to $k_B T$. However, they might be important for low-barrier processes, where the number of concerted reaction pathways becomes combinatorially more likely than single molecule processes. On the other hand, we also established that, due to the large number of dark states in these many-molecule polariton systems, nonadiabatic effects are not modified in any meaningful way under USC, at least for the model system explored. We provided a rationale behind this conclusion and discussed possibilities of seeing modifications in other systems where the excitonic and the electromagnetic modes anticross at large \mathbf{k} values.

Finally, it is worth noting that even though we considered an ultrastrong coupling regime ($\sqrt{N_{\mathbf{k}}(R)}$ reaches more than 10% of the maximum electronic energy gap in our model [29]), the system does not reach a Quantum Phase Transition (QPT) [51, 52]. In our model, this regime would require high density ($\sim 10^{10} \text{ molecules } \mu\text{m}^{-3}$) samples, keeping $\mu \approx 2 \text{ e\AA}$. The implications of this QPT on chemical reactivity have not been explored in this work, but are currently being studied in our group. To conclude, our present work highlights the limitations but also possibilities of USC in the context of control of chemical reactions using polaritonic systems.

VI. ACKNOWLEDGMENTS

R.F.R., J.C.A., and J.Y.Z. acknowledge support from the NSF CAREER award CHE-1654732. L.A.M.M is grateful to the support of the UC-Mexus CONACyT scholarship for doctoral studies. All authors acknowledge generous startup funds from UCSD. L.A.M.M. and J.Y.Z are thankful to Prof. Felipe Herrera for useful discussions.

VII. APPENDIX

In this appendix we outline the perturbative methodology that leads to the equations shown in the main text. Under the perturbative approach, it is convenient to express the perturbation in Eq. (11) in terms of

the Bogoliubov operators defined by Eq. (6). Notice that Eq. 11 introduces R -dependent exciton operators, while the zeroth order eigenstates (the polariton quasiparticles) are defined for all molecules at the configuration $R_{\mathbf{n},s} = 0$. It would be useful to find a relation $b_{\mathbf{n}_0,0}^\dagger(R) = f(b_{\mathbf{n}_0,0}^\dagger(0), b_{\mathbf{n}_0,0}(0))$ for any R , in order to carry out the aforementioned change of basis.

The function $f(b_{\mathbf{n}_0,0}^\dagger(0), b_{\mathbf{n}_0,0}(0))$ can be found by working on the diabatic basis (see Eq. 1). For any operator $b_{\mathbf{n},s}^\dagger(R)$, using $b_{\mathbf{n},s}^\dagger(R) = |e_{\mathbf{n},s}(R)\rangle\langle g_{\mathbf{n},s}(R)|$, we have

$$\begin{aligned} b_{\mathbf{n},s}^\dagger(R) &= [-\sin(\theta(R)/2)|\text{trans}_{\mathbf{n},s}\rangle + \cos(\theta(R)/2)|\text{cis}_{\mathbf{n},s}\rangle] \\ &\quad \times [\cos(\theta(R)/2)\langle\text{trans}_{\mathbf{n},s}| + \sin(\theta(R)/2)\langle\text{cis}_{\mathbf{n},s}|] \\ &= -\sin(\theta(R)/2)\cos(\theta(R)/2)b_{\mathbf{n},s}(0)b_{\mathbf{n},s}^\dagger(0) \quad (19) \\ &\quad - \sin(\theta(R)/2)^2 b_{\mathbf{n},s}(0) + \cos(\theta(R)/2)^2 b_{\mathbf{n},s}^\dagger(0) \\ &\quad + \cos(\theta(R)/2)\sin(\theta(R)/2)b_{\mathbf{n},s}^\dagger(0)b_{\mathbf{n},s}(0), \end{aligned}$$

where we used $b_{\mathbf{n},s}^\dagger(R_{eq}) = |\text{cis}_{\mathbf{n},s}\rangle\langle\text{trans}_{\mathbf{n},s}|$. In light of Eq. 19 we notice that the perturbation (11) in the second row produces chains with up to four exciton operators. In view of the delocalized nature of the zeroth-order eigenstates and the localized character of the exciton operators $b_{\mathbf{n},s}(0)$, we have that the matrix elements that appear in $E^{(2)}(R_{\mathbf{n}_0,0}, \tilde{\mathbf{O}}')$ are of the form $\langle G(\tilde{\mathbf{O}})|_d \xi_{\mathbf{k}_1}^i \xi_{\mathbf{k}_2}^j \dots \xi_{\mathbf{k}_{m+1}}^l F_m(b_{\mathbf{n}_0,0}^\dagger b_{\mathbf{n}_0,0}) Z(a_{\mathbf{k}}^\dagger, a_{\mathbf{k}})|G(\tilde{\mathbf{O}})\rangle_d \approx O(1/(N_x N_y)^{m/2})$, where $F_m(b_{\mathbf{n}_0,0}^\dagger b_{\mathbf{n}_0,0})$ stands for a chain with $1 \leq m \leq 4$ exciton operators and $Z(a_{\mathbf{k}}^\dagger, a_{\mathbf{k}})$ is a function of a single photonic operator. In the macroscopic limit $1 \ll N_x N_y$, we can neglect chains $F_m(b_{\mathbf{n}_0,0}^\dagger b_{\mathbf{n}_0,0}) Z(a_{\mathbf{k}}^\dagger, a_{\mathbf{k}})$ for $m \geq 2$. This leads to the simplification,

$$\begin{aligned} b_{\mathbf{n}_0,0}^\dagger(R) + b_{\mathbf{n}_0,0}(R) &\approx (\cos(\theta(R)/2)^2 - \sin(\theta(R)/2)^2) \\ &\quad \times (b_{\mathbf{n}_0,0}^\dagger(0) + b_{\mathbf{n}_0,0}(0)), \quad (20) \end{aligned}$$

and the perturbation acquires the simple form,

$$\begin{aligned} V(R) &\approx \sum_{\mathbf{k}, \mathbf{k}_1} D_{\mathbf{k}_1}^{\mathbf{n}_0,0} \left(\cos(\theta(R)) g_{\mathbf{k}}^{\mathbf{n}_0,0}(R) - g_{\mathbf{k}}^{\mathbf{n}_0,0}(0) \right) \\ &\quad \times \left(b_{\mathbf{k}_1}(0) a_{\mathbf{k}}^\dagger + b_{\mathbf{k}_1}^\dagger(0) a_{\mathbf{k}}^\dagger + a_{\mathbf{k}} b_{\mathbf{k}_1}(0) + b_{\mathbf{k}_1}^\dagger(0) a_{\mathbf{k}} \right). \quad (21) \end{aligned}$$

To write this last expression in terms of the Bogoliubov operators $\{\xi_{\mathbf{k}_1}^{i\dagger}(0)\xi_{\mathbf{k}_2}^{j\dagger}(0)\}$ we start from the transformation $\vec{\xi} = T\vec{b}$:

$$\begin{bmatrix} \xi_{\mathbf{k}}^L(0) \\ \xi_{\mathbf{k}}^U(0) \\ \xi_{-\mathbf{k}}^{L\dagger}(0) \\ \xi_{-\mathbf{k}}^{U\dagger}(0) \end{bmatrix} = \begin{bmatrix} \alpha_{\mathbf{k}}^L & \beta_{\mathbf{k}}^L & \gamma_{\mathbf{k}}^L & \delta_{\mathbf{k}}^L \\ \alpha_{\mathbf{k}}^U & \beta_{\mathbf{k}}^U & \gamma_{\mathbf{k}}^U & \delta_{\mathbf{k}}^U \\ \gamma_{\mathbf{k}}^{L*} & \delta_{\mathbf{k}}^{L*} & \alpha_{\mathbf{k}}^{L*} & \beta_{\mathbf{k}}^{L*} \\ \gamma_{\mathbf{k}}^{U*} & \delta_{\mathbf{k}}^{U*} & \alpha_{\mathbf{k}}^{U*} & \beta_{\mathbf{k}}^{U*} \end{bmatrix} \begin{bmatrix} a_{\mathbf{k}} \\ b_{\mathbf{k}}(0) \\ a_{-\mathbf{k}}^\dagger \\ b_{-\mathbf{k}}^\dagger(0) \end{bmatrix}. \quad (22)$$

From the matrix representation of the normalization $|\alpha_{\mathbf{k}}^i|^2 + |\beta_{\mathbf{k}}^i|^2 - |\gamma_{\mathbf{k}}^i|^2 - |\delta_{\mathbf{k}}^i|^2 = 1$ [33], it follows that,

$$T I_- T^\dagger = I_-, \quad (23)$$

where

$$I_- = \begin{bmatrix} 1 & 0 & 0 & 0 \\ 0 & 1 & 0 & 0 \\ 0 & 0 & -1 & 0 \\ 0 & 0 & 0 & -1 \end{bmatrix}. \quad (24)$$

We also have that $T^{-1} = I_- T^\dagger I_-$ and that

$$T^{-1} = \begin{bmatrix} \alpha_{\mathbf{k}}^{L*} & \alpha_{\mathbf{k}}^{U*} & -\gamma_{\mathbf{k}}^L & -\gamma_{\mathbf{k}}^U \\ \beta_{\mathbf{k}}^{L*} & \beta_{\mathbf{k}}^{U*} & -\delta_{\mathbf{k}}^L & -\delta_{\mathbf{k}}^U \\ -\gamma_{\mathbf{k}}^{L*} & -\gamma_{\mathbf{k}}^{U*} & \alpha_{\mathbf{k}}^L & \alpha_{\mathbf{k}}^U \\ -\delta_{\mathbf{k}}^{L*} & -\delta_{\mathbf{k}}^{U*} & \beta_{\mathbf{k}}^L & \beta_{\mathbf{k}}^U \end{bmatrix}. \quad (25)$$

Using Eq. 25, we can readily evaluate $\vec{b} = T^{-1}\vec{\xi}$. From this relationship, the change of the localized operators to the Bogoliubov basis is accomplished. Finally, the matrix elements to compute $E^{(2)}(R_{\mathbf{n}_0,0}, \tilde{\mathbf{O}}')$ can be evaluated by means of Wick's theorem,

$$\begin{aligned} \langle G(\tilde{\mathbf{O}})|_d \xi_{\mathbf{k}_1}^l \xi_{\mathbf{k}_2}^n \xi_{\mathbf{k}'}^{i\dagger} \xi_{\mathbf{k}'}^{j\dagger} |G(\tilde{\mathbf{O}})\rangle_d &= \delta_{l,j} \delta_{\mathbf{k}_1, \mathbf{k}'} \delta_{i,n} \delta_{\mathbf{k}_2, \mathbf{k}} \quad (26) \\ &\quad + \delta_{n,j} \delta_{\mathbf{k}_2, \mathbf{k}'} \delta_{m,i} \delta_{\mathbf{k}_1, \mathbf{k}}, \end{aligned}$$

leading to Eq. 13.

-
- [1] Kim, M.-K.; Sim, H.; Yoon, S. J.; Gong, S.-H.; Ahn, C. W.; Cho, Y.-H.; Lee, Y.-H. *Nano Letters* **2015**, *15*, 4102–4107, PMID: 26010266.
 - [2] Gonzalez-Ballesteros, C.; Feist, J.; Moreno, E.; Garcia-Vidal, F. J. *Phys. Rev. B - Condens. Matter Mater. Phys.* **2015**, *92*, 1–5.
 - [3] Feist, J.; Garcia-Vidal, F. J. *Phys. Rev. Lett.* **2015**, *114*, 1–5.
 - [4] Herrera, F.; Spano, F. C. *Phys. Rev. Lett.* **2016**, *116*, 1–6.
 - [5] et al. Kasprzak, J. *Nature* **2006**, *443*, 409–414.
 - [6] Gerace, D.; Carusotto, I. *Phys. Rev. B - Condens. Matter Mater. Phys.* **2012**, *86*, 1–12.
 - [7] Nguyen, H. S.; Gerace, D.; Carusotto, I.; Sanvitto, D.; Galopin, E.; Lemaître, a.; Sagnes, I.; Bloch, J.; Amo, a. *Phys. Rev. Lett.* **2015**, *114*, 1–5.
 - [8] Strashko, A.; Keeling, J. *Phys. Rev. A* **2016**, *94*, 023843.
 - [9] del Pino, J.; Feist, J.; Garcia-Vidal, F. J. *The Journal of Physical Chemistry C* **2015**, *119*, 29132–29137.
 - [10] Herrera, F.; Spano, F. C. *Phys. Rev. A* **2017**, *95*, 053867.
 - [11] Melnikau, D.; Esteban, R.; Savateeva, D.; Sánchez-Iglesias, A.; Grzelczak, M.; Schmidt, M. K.; Liz-Marzán, L. M.; Aizpurua, J.; Rakovich, Y. P. *The Journal of Physical Chemistry Letters* **2016**, *7*, 354–362, PMID: 26726134.
 - [12] Del Pino, J.; Feist, J.; García-Vidal, F. J.; García-Ripoll, J. J. *Phys. Rev. Lett.* **2014**, *112*, 1–5.
 - [13] Hartmann, M. J.; Brandao, F. G. S. L.; Plenio, M. B. *Nat. Phys.* **2006**, *2*, 849–855.

- [14] Raimond, J. M.; Brune, M.; Haroche, S. *Rev. Mod. Phys.* **2001**, *73*, 565–582.
- [15] Bellessa, J.; Bonnand, C.; Plenet, J. C.; Mugnier, J. *Phys. Rev. Lett.* **2004**, *93*, 036404.
- [16] Laussy, F. P.; del Valle, E.; Tejedor, C. *Phys. Rev. Lett.* **2008**, *101*, 083601.
- [17] Lidzey, D. G.; Bradley, D. D. C.; Virgili, T.; Armitage, A.; Skolnick, M. S.; Walker, S. *Phys. Rev. Lett.* **1999**, *82*, 3316–3319.
- [18] Tischler, J. R.; Bradley, M. S.; Bulović, V.; Song, J. H.; Nurmikko, A. *Phys. Rev. Lett.* **2005**, *95*, 036401.
- [19] Hobson, P. A.; Barnes, W. L.; Lidzey, D. G.; Gehring, G. A.; Whittaker, D. M.; Skolnick, M. S.; Walker, S. *Applied Physics Letters* **2002**, *81*, 3519–3521.
- [20] Bellessa, J.; Bonnand, C.; Plenet, J. C.; Mugnier, J. *Phys. Rev. Lett.* **2004**, *93*, 036404.
- [21] Salomon, A.; Genet, C.; Ebbesen, T. W. *Angewandte Chemie - Int. Ed.* **2009**, *48*, 8748–8751.
- [22] Hutchison, J. a.; Schwartz, T.; Genet, C.; Devaux, E.; Ebbesen, T. W. *Angew. Chemie - Int. Ed.* **2012**, *51*, 1592–1596.
- [23] Thomas, A.; George, J.; Shalabney, A.; Dryzhakov, M.; Varma, S. J.; Moran, J.; Chervy, T.; Zhong, X.; Devaux, E.; Genet, C.; Hutchison, J. a.; Ebbesen, T. W. *Angew. Chemie - Int. Ed.* **2016**, 11634–11638.
- [24] Galego, J.; Garcia-Vidal, F. J.; Feist, J. *Nature Communications* **2016**, *7*.
- [25] Flick, J.; Ruggenthaler, M.; Appel, H.; Rubio, A. *Proceedings of the National Academy of Sciences* **2017**, *114*, 3026–3034.
- [26] Galego, J.; Garcia-Vidal, F. J.; Feist, J. *Phys. Rev. X* **2015**, *5*, 1–14.
- [27] Chikkaraddy, R.; de Nijs, B.; Benz, F.; Barrow, S. J.; Scherman, O. a.; Rosta, E.; Demetriadou, A.; Fox, P.; Hess, O.; Baumberg, J. J. *Nature* **2016**, *535*, 127–130.
- [28] Cwik, J. a.; Kirton, P.; De Liberato, S.; Keeling, J. *Phys. Rev. A - At. Mol. Opt. Phys.* **2016**, *93*, 1–12.
- [29] Moroz, A. *Annals of Physics* **2014**, *340*, 252 – 266.
- [30] Wilson, C. M.; Johansson, G.; Pourkabirian, A.; Simoen, M.; Johansson, J. R.; Duty, T.; Nori, F.; Delsing, P. *Nature* **2011**, *479*, 376–379.
- [31] Stassi, R.; Ridolfo, A.; Di Stefano, O.; Hartmann, M. J.; Savasta, S. *Phys. Rev. Lett.* **2013**, *110*, 243601.
- [32] Niemczyk, T.; Deppe, F.; Huebl, H.; Menzel, E. P.; Hocke, F.; Schwarz, M. J.; Garcia-Ripoll, J. J.; Zueco, D.; Hümmer, T.; Solano, E.; Marx, a.; Gross, R. *Nat. Phys.* **2010**, *6*, 772.
- [33] Ciuti, C.; Bastard, G.; Carusotto, I. *Phys. Rev. B* **2005**, *72*, 115303.
- [34] Todorov, Y.; Andrews, A. M.; Colombelli, R.; De Liberato, S.; Ciuti, C.; Klang, P.; Strasser, G.; Sirtori, C. *Phys. Rev. Lett.* **2010**, *105*, 196402.
- [35] Schwartz, T.; Hutchison, J. A.; Genet, C.; Ebbesen, T. W. *Phys. Rev. Lett.* **2011**, *106*, 196405.
- [36] George, J.; Chervy, T.; Shalabney, A.; Devaux, E.; Hiura, H.; Genet, C.; Ebbesen, T. W. *Physical Review Letters* **2016**, *117*, 153601.
- [37] Hoki, K.; Brumer, P. *Chem. Phys. Lett.* **2009**, *468*, 23–27.
- [38] Yuen-Zhou, J.; Saikin, S. K.; Zhu, T. H.; Onbasli, M. C.; Ross, C. a.; Bulovic, V.; Baldo, M. a. *Nat. Commun.* **2016**, *7*, 11783.
- [39] González-Tudela, a.; Huidobro, P. a.; Martín-Moreno, L.; Tejedor, C.; Garcia-Vidal, F. J. *Phys. Rev. Lett.* **2013**, *110*, 1–5.
- [40] Garraway, B. M. *Philosophical Transactions of the Royal Society of London A: Mathematical, Physical and Engineering Sciences* **2011**, *369*, 1137–1155.
- [41] Novotny, L.; Hecht, B. *Principles of Nano-Optics*; Cambridge University Press, 2012.
- [42] Törmä, P.; Barnes, W. L. *Rep. Prog. Phys.* **2015**, *78*, 013901.
- [43] Tassone, F.; Yamamoto, Y. *Phys. Rev. B* **1999**, *59*, 10830–10842.
- [44] Bethe, H. A.; Brown, L. M.; Stehn, J. R. *Phys. Rev.* **1950**, *77*, 370–374.
- [45] Rowland, R. S.; Taylor, R. *The Journal of Physical Chemistry* **1996**, *100*, 7384–7391.
- [46] Galego, J.; Garcia-Vidal, F. J.; Feist, J. *arXiv preprint arXiv:1704.07261* **2017**,
- [47] Kowalewski, M.; Bennett, K.; Mukamel, S. *J. Phys. Chem. Lett.* **2016**, *7*, 2050–2054.
- [48] Bennett, K.; Kowalewski, M.; Mukamel, S. *Faraday Discuss.* **2016**, 10.1039/C6FD00095A.
- [49] Bohm, A.; Mostafadeh, A.; Koizumi, H.; Niu, Q.; Zwanziger, J. *The Geometric Phase in Quantum Systems*, 1st ed.; Springer: New York, 2003.
- [50] Jenkins, M.; Hümmer, T.; Martínez-Pérez, M. J.; García-Ripoll, J.; Zueco, D.; Luis, F. *New J. Phys.* **2013**, *15*.
- [51] Emary, C.; Brandes, T. *Phys. Rev. Lett.* **2003**, *90*, 044101.
- [52] Li, Y.; Wang, Z. D.; Sun, C. P. *Phys. Rev. A - At. Mol. Opt. Phys.* **2006**, *74*, 1–5.